

Term Project (1)

- The term project is carried out in teams of 2-3 students
- One-page project proposal (due date Dec. 10, 2020)
 - The problem description
 - Background, previous work, motivation
 - Methods
 - Assumption(s), proposed flowchart or steps
 - Possible results
 - References
 - Books, papers, websites
- Project demo (Dec 28, Dec 31, 2020 & Jan 4, Jan 7, 2021)
- Final report (Jan 18, 2021)
 - The final report (4-6 pages) should extend your proposal to include detailed methods, experimental results and discussion

Term Project (2)

- Project scope
 - To address image processing problems while manipulating the collection of color images
- Suggested topics
 - Enhancement
 - Color & detail transfer, super-resolution
 - Image fusion, exposure fusion
 - Restoration
 - Deblurring, de-weathering
 - Editing
 - Retargeting, inpainting, style transfer
 - Re-focusing
 - Any other topics related to the theme of this course

Color & Contrast Transfer (1)

- Color transfer basic

- To make a synthetic image with another image's look and feel

- Step1:

- Converting RGB to a decorrelated color space $l\alpha\beta$

$$\begin{bmatrix} L \\ M \\ S \end{bmatrix} = \begin{bmatrix} 0.3811 & 0.5783 & 0.0402 \\ 0.1967 & 0.7244 & 0.0782 \\ 0.0241 & 0.1288 & 0.8444 \end{bmatrix} \begin{bmatrix} R \\ G \\ B \end{bmatrix}$$

Decorrelation allows us to treat the 3 color channels separately

$$\begin{aligned} L &= \log L \\ M &= \log M \\ S &= \log S \end{aligned} \quad \begin{bmatrix} l \\ \alpha \\ \beta \end{bmatrix} = \begin{bmatrix} \frac{1}{\sqrt{3}} & 0 & 0 \\ 0 & \frac{1}{\sqrt{6}} & 0 \\ 0 & 0 & \frac{1}{\sqrt{2}} \end{bmatrix} \begin{bmatrix} 1 & 1 & 1 \\ 1 & 1 & -2 \\ 1 & -1 & 0 \end{bmatrix} \begin{bmatrix} L \\ M \\ S \end{bmatrix}$$

- E. Reinhard, M. Ashikhmin, B. Gooch, and P. Shirley, "Color transfer between images," *IEEE Comput. Graph. Appl.*, Vol. 21, No. 5, pp. 34–41, 2001.

Color & Contrast Transfer (2)

- Color transfer basic

- Step 2:

- Computing the means and standard deviations for source and target images along each of the $l\alpha\beta$ space
- Adjusting the means and standard deviations of the synthetic image

$$\begin{aligned} l^* &= l - \langle l \rangle & l' &= \frac{\sigma_t^l}{\sigma_s^l} l^* \\ \alpha^* &= \alpha - \langle \alpha \rangle & \alpha' &= \frac{\sigma_t^\alpha}{\sigma_s^\alpha} \alpha^* \\ \beta^* &= \beta - \langle \beta \rangle & \beta' &= \frac{\sigma_t^\beta}{\sigma_s^\beta} \beta^* \end{aligned}$$

$$\begin{aligned} l'' &= l' + \langle l \rangle \\ \alpha'' &= \alpha' + \langle \alpha \rangle \\ \beta'' &= \beta' + \langle \beta \rangle \end{aligned}$$

Color & Contrast Transfer (3)

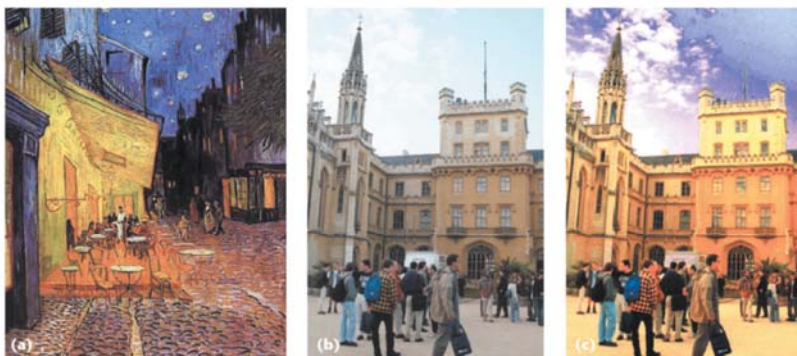
- Color transfer basic
 - Step 3:
 - Converting the color back to RGB

$$\begin{bmatrix} \mathbf{L} \\ \mathbf{M} \\ \mathbf{S} \end{bmatrix} = \begin{bmatrix} 1 & 1 & 1 \\ 1 & 1 & -1 \\ 1 & -2 & 0 \end{bmatrix} \begin{bmatrix} \frac{\sqrt{3}}{3} & 0 & 0 \\ 0 & \frac{\sqrt{6}}{6} & 0 \\ 0 & 0 & \frac{\sqrt{2}}{2} \end{bmatrix} \begin{bmatrix} l \\ \alpha \\ \beta \end{bmatrix}$$

$$\begin{bmatrix} R \\ G \\ B \end{bmatrix} = \begin{bmatrix} 4.4679 & -3.5873 & 0.1193 \\ -1.2186 & 2.3809 & -0.1624 \\ 0.0497 & -0.2439 & 1.2045 \end{bmatrix} \begin{bmatrix} L \\ M \\ S \end{bmatrix}$$

Color & Contrast Transfer (4)

- Color transfer & color correction



4 Using swatches. We applied (a) the atmosphere of Vincent van Gogh's *Cafe Terrace on the Place du Forum, Arles, at Night* (Arles, September 1888, oil on canvas; image from the Vincent van Gogh Gallery, <http://www.vangoghgallery.com>) to (b) a photograph of Lednice Castle near Brno in the Czech Republic. (c) We matched the blues of the sky in both images, the yellows of the cafe and the castle, and the browns of the tables at the cafe and the people at the castle separately.



6 Color correction. Top to bottom: renderings using red, tungsten, and blue light sources. Left to right: original image, corrected using gray world assumption in $l\alpha\beta$ space. The averages were browsed to more closely resemble Pattanaik's color correction results.⁷ (Images courtesy of Mark Fairchild.)

- E. Reinhard, M. Ashikhmin, B. Gooch, and P. Shirley, "Color transfer between images," *IEEE Comput. Graph. Appl.*, Vol. 21, No. 5, pp. 34–41, 2001.

Color & Contrast Transfer (5)

$$h_{T(u)} \simeq f.$$

If f is a constant distribution on the range of u , one gets the well known *histogram equalization*. More generally, if f is the gray level distribution h_v of a style image v , then $T = H_v^{-1} \circ H_u$ is called *histogram specification*.

The resulting regularization of the image $T(u)$, referred to as *Transportation Map Regularization (TMR)*, is then defined as $\text{TMR}_u(T(u)) := u + Y_u \mathcal{M}(u)$. Now, observe that this formulation can be divided in two terms :

$$\text{TMR}_u(T(u)) = \underbrace{Y_u(T(u))}_{\text{filtering of image } T(u)} + \underbrace{u - Y_u(u)}_{\text{source image detail}}. \quad (4)$$



(a) Source image (Auguste Renoir, *Le déjeuner des Canotiers*, 1881).



(b) Style image (Paul Gauguin, *Mahana no atua - le jour de Dieu*, 1894).



(c) Color transfer.



(d) Iterated TRM filter.



(i) Source image.



(j) Style image.



(k) Color transfer + regaining with approach of [6].



(l) Iterated TRM filter.

- J. Rabin, J. Delon, and Y. Gousseau, "Regularization of transportation maps for color and contrast transfer," *Proc. ICIP*, 2010.

Detail Transfer

- Natural ambient illumination
- Visible noises

- Noise-free
- With details
- Artifacts (red eye, harsh shadows)

we modify the basic bilateral filter to compute the edge-stopping function g_r , using the flash image F instead of A . We call this technique the *joint bilateral filter*:

$$A_p^{NR} = \frac{1}{k(p)} \sum_{p' \in \Omega} g_d(p' - p) g_r(F_p - F_{p'}) A_{p'}, \quad (4)$$

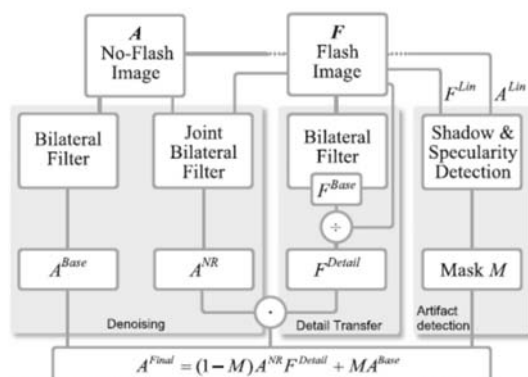


Figure 3: Overview of our algorithms for denoising, detail transfer, and flash artifact detection.

$$F^{Detail} = \frac{F + \epsilon}{F^{Base} + \epsilon}$$



Figure 1: This candlelit setting from the wine cave of a castle is difficult to photograph due to its low light nature. A flash image captures the high-frequency texture and detail, but changes the overall scene appearance to cold and gray. The no-flash image captures the overall appearance of the warm candlelight, but is very noisy. We use the detail information from the flash image to both reduce noise in the no-flash image and sharpen its detail. Note the smooth appearance of the brown leather sofa and crisp detail of the bottles. For full-sized images, please see the supplemental DVD or the project website <http://research.microsoft.com/projects/FlashNoFlash>.

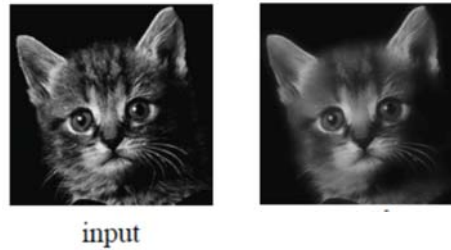
- G. Petschnigg, M. Agrawala, H. Hoppe, R. Szeliski, M. Cohen, and K. Toyama, "Digital photography with flash and no-flash image pairs," in *ACM SIGGRAPH*, 2004.

Guided Image Filter (1)

- Edge-preserving filtering

- Guide = input

- $I \equiv p$



- Structure-transferring filtering



- Kaiming He, Jian Sun, and Xiaoou Tang, "Guided Image Filtering," *IEEE Trans. PAMI*, vol. 35, no. 6, June 2013, pp. 1397-1409.

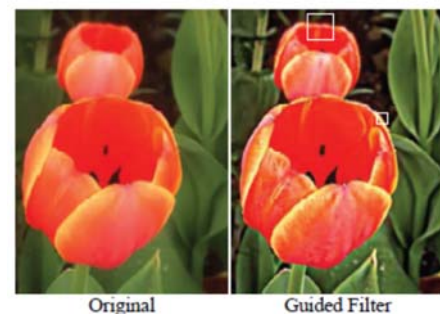
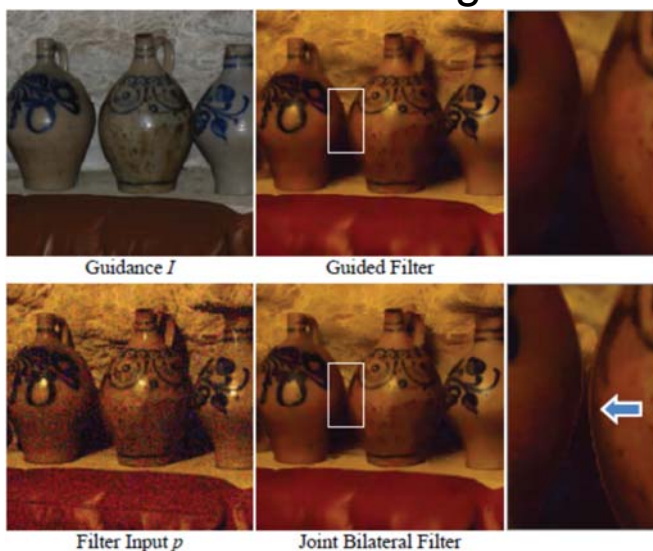
Guided Image Filter (2)

- Detail enhancement

- Detail $d = p - q$

- Enhanced result = $q + \text{boosted } d$

- Flash/Non-flash denoising



Single-Image SuperResolution (1)

- Problem formulation
 - The low resolution image L is assumed to be generated from H
 - $L = (H * B) \downarrow_{scale}$
 - B : blur
 - \downarrow : subsampling process
 - Each pixel $p = (x, y)$ in L induces one constraint
 - $L(p) = (H * B)(q) = \sum_{q_i \in Support(B)} H(q) B(q_i - q)$
- To recover H from a single-image L
 - #constraints induced by $L < \#unknowns$ in H
 - Under-determined

Single-Image SuperResolution (2)

- Goal
 - To recover missing high-resolution details that are not found in low-resolution images
- Assumption
 - Patches in a natural image tend to recur inside the image
 - Within the same scale & across different scales
 - D. Glasner, S. Bagon, and M. Irani, “Super-resolution from a Single Image,” *Proc. ICCV*, 2009.
<http://www.wisdom.weizmann.ac.il/~vision/SingleImageSR.html>

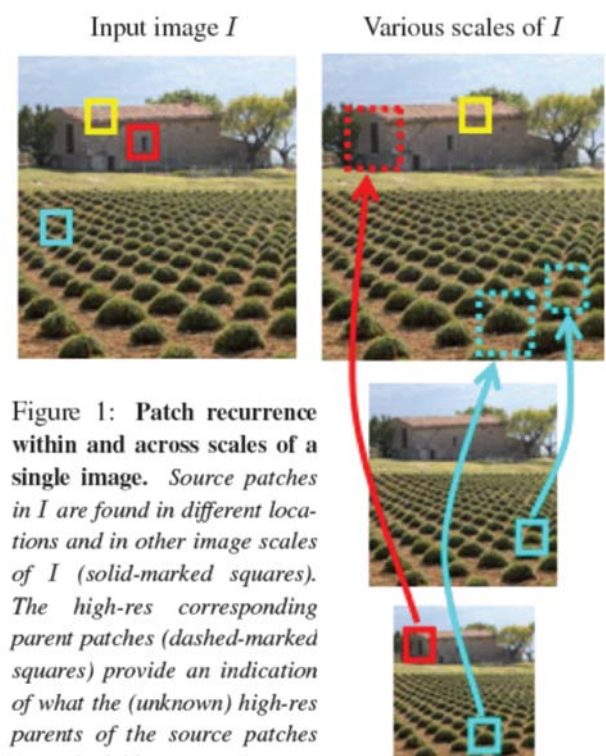


Figure 1: Patch recurrence within and across scales of a single image. Source patches in I are found in different locations and in other image scales of I (solid-marked squares). The high-res corresponding parent patches (dashed-marked squares) provide an indication of what the (unknown) high-res parents of the source patches might look like.

Single-Image SuperResolution (3)

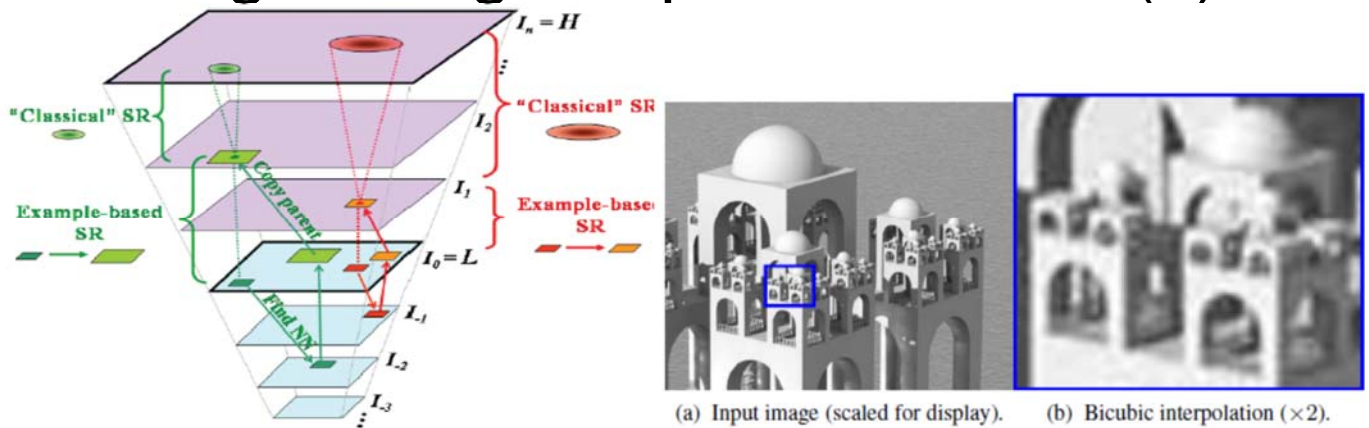


Figure 4: Combining Example-based SR constraints with Classical SR constraints in a single unified computational framework. Patches in the input low-res image L (dark red and dark green patches) are searched for in the down-scaled versions of L (blue-marked images). When a similar patch is found, its parent patch (light red and light green) is copied to the appropriate location in the unknown high-resolution image (purple images) with the appropriate gap in scale. A 'learned' (copied) high-res patch induces classical SR linear constraints on the unknown high-res intensities in the target high-res H . The support of the corresponding blur kernels (red and green ellipses) are determined by the residual gaps in scale between the resolution levels of the 'learned' high-res patches and the target resolution level of H . Note that for different patches found in different scale gaps, the corresponding blur kernels (red and green ellipses) will accordingly have different supports. (See text for more details.)



(d) Unified single-image SR ($\times 2$).

Single-Image SuperResolution (4)

- Goal
 - Extending the patch search space by allowing geometric variations

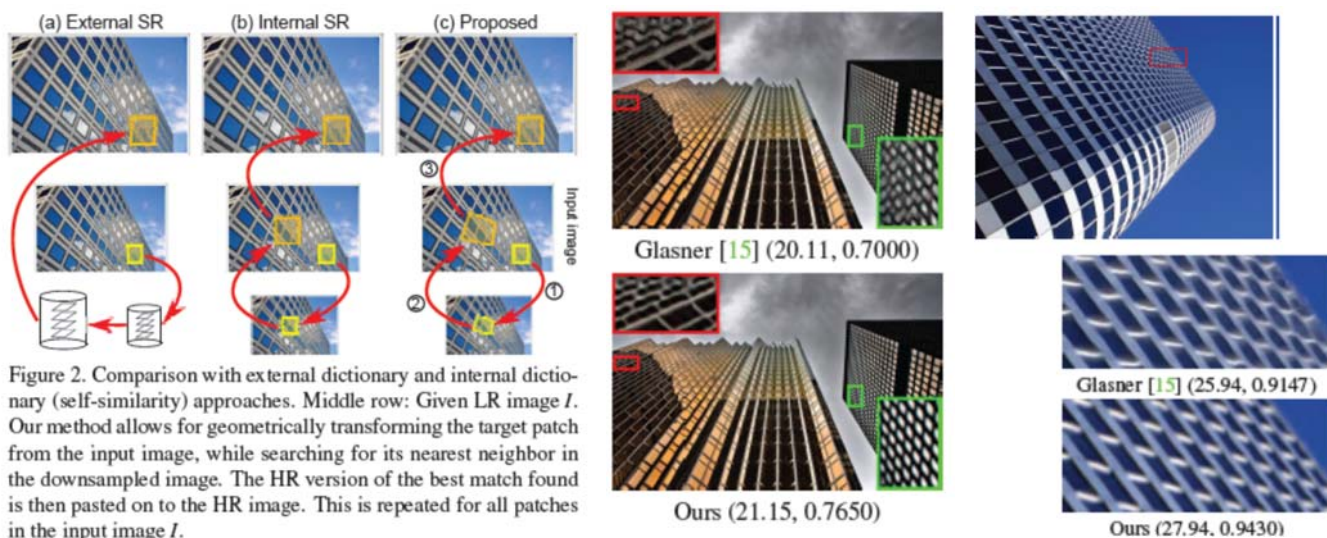


Figure 2. Comparison with external dictionary and internal dictionary (self-similarity) approaches. Middle row: Given LR image I . Our method allows for geometrically transforming the target patch from the input image, while searching for its nearest neighbor in the downsampled image. The HR version of the best match found is then pasted on to the HR image. This is repeated for all patches in the input image I .

- Jia-Bin Huang, Abhishek Singh, and Narendra Ahuja, "Single Image Super-resolution from Transformed Self-Exemplars," in *Proc. CVPR*, 2015.

SuperResolution for Structured Edges

- Method

- Finding a transform that maps the image to a domain where the edges are mostly aligned vertically & horizontally
- Super resolve under constraints on the transformed image
 - The edge structure is approximately low rank

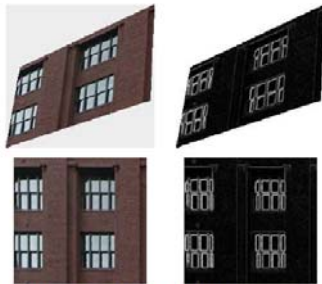
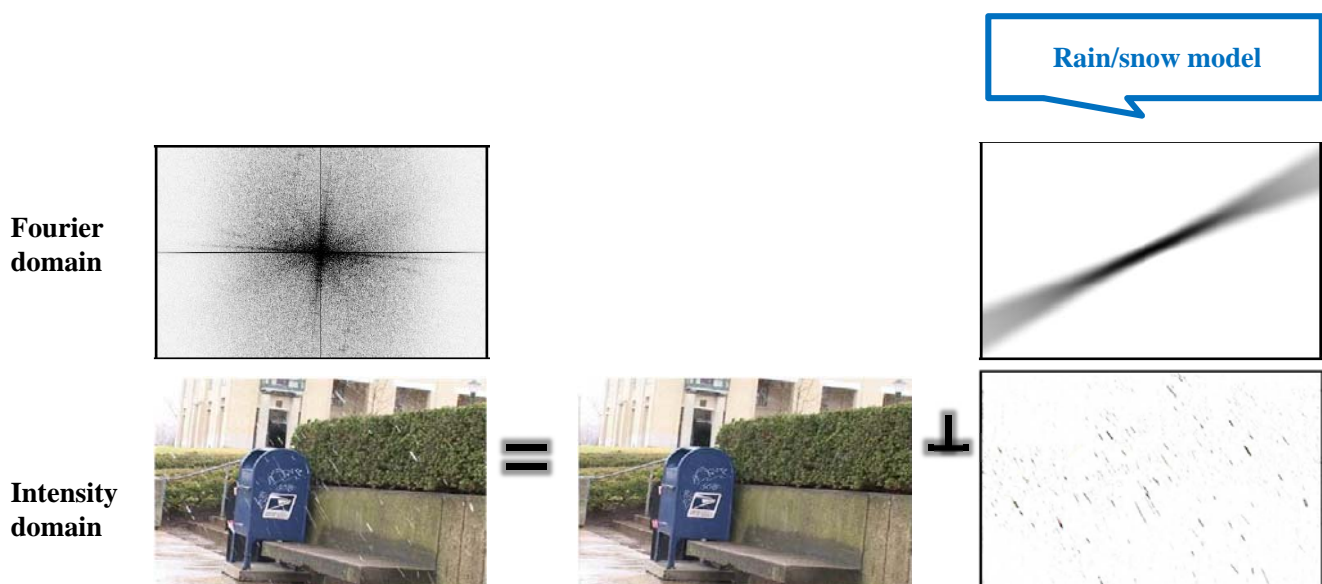


Figure 1. Image of a building façade (top left) and its gradient (top right) along with their low-rank representation (bottom).



- C. Fernandez-Granda, and E.J. Candes, “Super-resolution via Transform-invariant Group-sparse Regularization,” in *Proc. ICCV*, 2013.
www.stanford.edu/~cfgranda/TI_DTV_code.zip

Rain/Snow Removal



- P. C. Barnum, S. Narasimhan, T. Kanade, “Analysis of Rain and Snow in Frequency Space,” *International Journal of Computer Vision*, 2009.
<http://www.cs.cmu.edu/~pbarnum/rain/rainAndSnow.html>

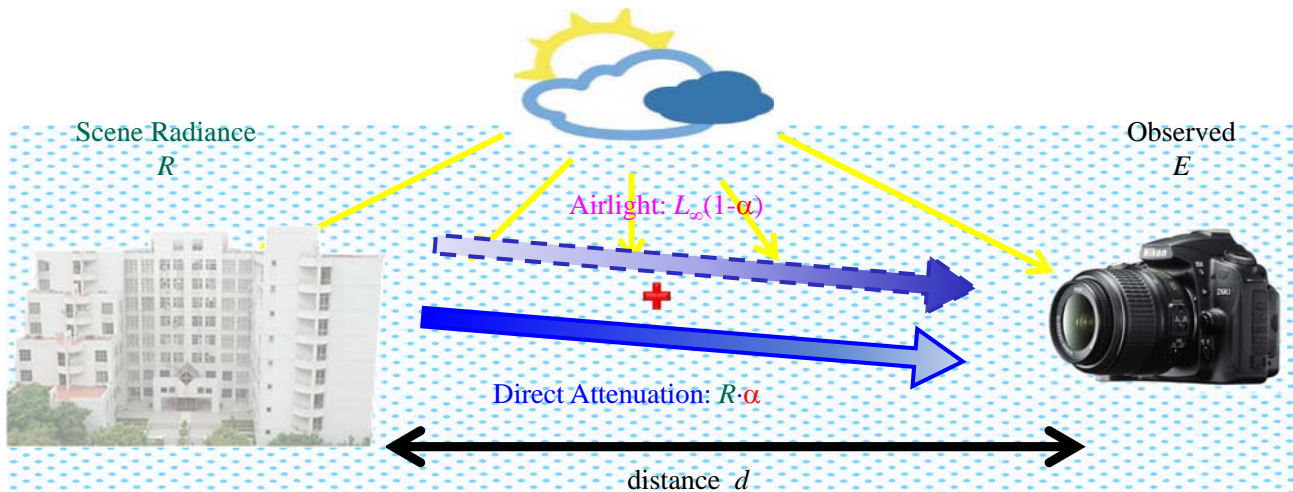
Image Dehazing

- Hazing model

Observed hazy image = Direct Attenuation + Airlight

$$\begin{aligned}
 E(x, y) &= R(x, y)e^{-\beta d(x, y)} + L_{\infty}(1 - e^{-\beta d(x, y)}) \\
 &= R(x, y)\alpha(x, y) + L_{\infty}(1 - \alpha(x, y))
 \end{aligned}$$

α : transmission



Single Image Dehazing using Dark Channel Prior (1)

- Dark channel prior

- Pixels in hazy-free images often have very low intensity in at least one color (RGB) channel

$$\frac{E(x, y)}{L_{\infty}} = \frac{R(x, y)}{L_{\infty}} \alpha(x, y) + (1 - \alpha(x, y))$$

$$\min_{\text{local patch}} \left\{ \min_c \left\{ \frac{E^c(x, y)}{L_{\infty}^c} \right\} \right\} = \alpha(x, y) \min_{\text{local patch}} \left\{ \min_c \left\{ \frac{R^c(x, y)}{L_{\infty}^c} \right\} \right\} + (1 - \alpha(x, y))$$

Dark channel, 0

- Then

$$\alpha(x, y) = 1 - \min_{\text{local patch}} \left\{ \min_c \left\{ \frac{E^c(x, y)}{L_{\infty}^c} \right\} \right\}$$

- K. He, J. Sun, and X. Tang, "Single Image Haze Removal Using Dark Channel Prior," *IEEE Trans. PAMI*, vol. 33, no. 12, Aug. 2010, pp. 2341-2353.

Single Image Dehazing using Dark Channel Prior (2)

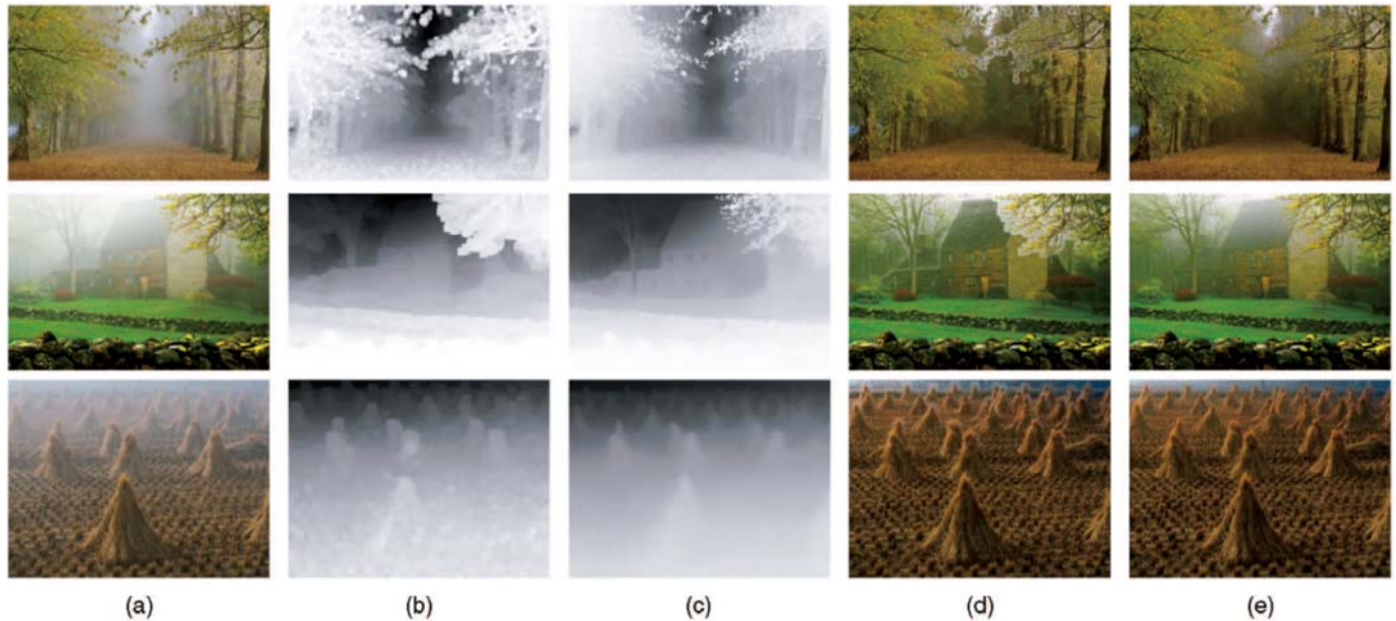


Fig. 6. Haze removal. (a) Input hazy images. (b) Estimated transmission maps before soft matting. (c) Refined transmission maps after soft matting (d), (e) Recovered images using (b) and (c), respectively.

Single Image Dehazing via Optimal Transmission (1)

- Theoretical bounds of scene transmission
 - $E(x, y) = R(x, y)\alpha(x, y) + L_\infty(1 - \alpha(x, y))$
 - From 3 observations
 - $R(x, y) \geq 0$
 - $0 \leq \alpha(x, y) \leq 1$
 - $\alpha(x, y)$ is independent of color channels
 - We have
 - $E(x, y) \geq L_\infty(1 - \alpha(x, y))$
 - $\Rightarrow \alpha(x, y) \geq 1 - \frac{E(x, y)}{L_\infty}$ Same as dark channel prior
 - $\Rightarrow 1 - \min_c \left\{ \frac{E^c(x, y)}{L_\infty} \right\} \leq \alpha(x, y) \leq 1$
 - Yi-Hsuan Lai, Yi-Lei Chen, Chuan-Ju Chiou, and Chiou-Ting Hsu, "Single Image Dehazing Via Optimal Transmission Map Under Scene Priors," *IEEE Trans. Circuits and Systems for Video Technology*, vol. 25, no. 1, Jan. 2015, pp. 1-14.

Single Image Dehazing via Optimal Transmission (2)

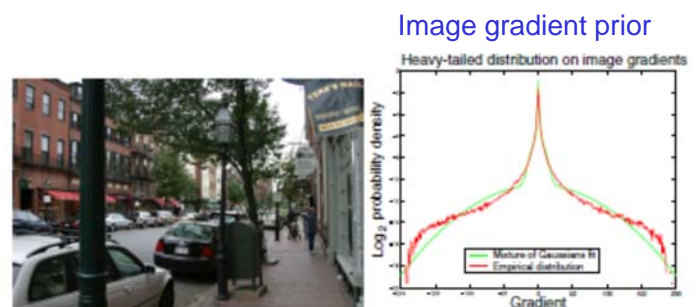
Proposed

Dark channel prior



Single Image Deblurring (1)

- Blind deconvolution
 - Both the blur kernel h & latent image f are unknown
 - Ill-posed problem
 - Because many different pairs h and f give rise to the same g
- Assumptions
 - Natural image statistics
 - Sparsity of image gradients
 - Internal patch recurrence
 - ...



R. Fergus et al., "Removing Camera Shake from a Single Photograph," *ACM Transactions on Graphic*, 2006.

Figure 2: Left: A natural scene. Right: The distribution of gradient magnitudes within the scene are shown in red. The y-axis has a logarithmic scale to show the heavy tails of the distribution. The mixture of Gaussians approximation used in our experiments is shown in green.

Single Image Deblurring (2)

- Iterative minimization of errors caused by
 - Inaccurate blur kernel
 - Image noise

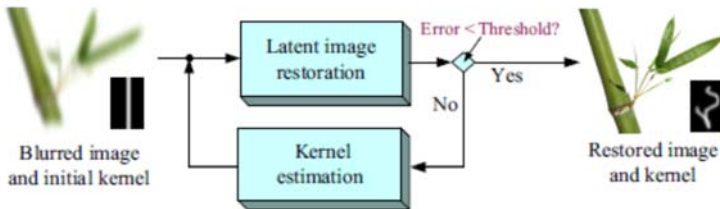


Figure 5 Overview of our algorithm. Given an observed blurred image and an initial kernel, our proposed method iteratively estimates the latent image and refines the blur kernel until convergence.



- Qi Shan, Jiaya Jia and Aseem Agarwala, "High-quality Motion Deblurring from a Single Image," *ACM SIGGRAPH*, 2008.
http://www.cse.cuhk.edu.hk/~leojia/projects/motion_deblurring/index.html

Single Image Deblurring (3)

- Observation
 - Light streaks in low-light images contain rich blur information



Figure 1. Deblurring low-light images. (a) A real example. (b) A cropped region from (a). (c-e) Cropped deblurring results of Cho and Lee [2], Xu and Jia [19], and our approach, respectively. Please refer to the supplementary material for full resolution images and complete results.

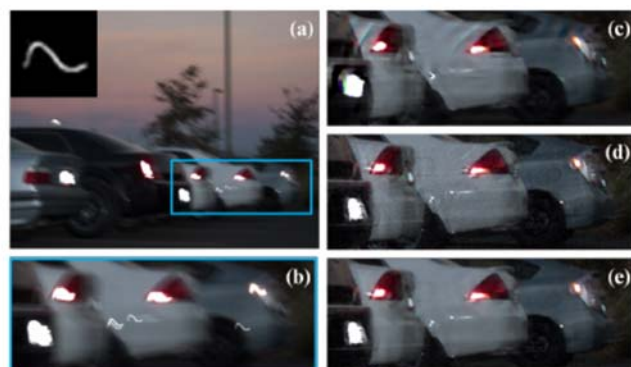


Figure 3. Non-blind deconvolution of a synthetic example. (a) Input image with the ground truth blur kernel. (b) A cropped region from (a). (c-e) Cropped deconvolution results of Cho et al. [3], Whyte et al. [17] and our approach, respectively. Please refer to the supplementary material for complete results.

- Z. Hu et.al, "Deblurring Low-Light Images with Light Streaks," in *Proc. CVPR*, 2014.

Deblurring Using Dark Channel Prior (1)

- Assumption
 - Dark channel of original images are sparse
- Observation
 - Dark channels of blurred images are less sparse

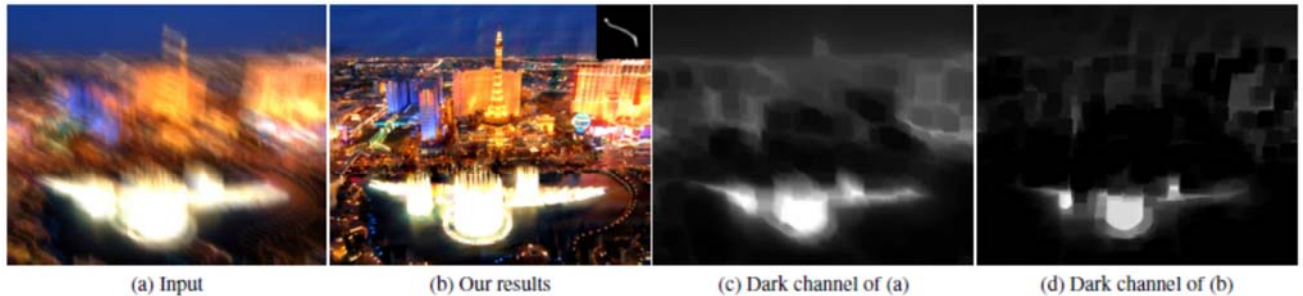


Figure 1. Deblurring result on a challenging low-light image. The blur process makes the dark channel of the blurred image less sparse (c). Enforcing sparsity on the dark channel of the recovered image favors clean images over blurred ones.

- Jinshan Pan, Deqing Sun, Hanspeter Pfister and Ming-Hsuan Yang, Blind Image Deblurring Using Dark Channel Prior, CVPR 2016.

Deblurring Using Dark Channel Prior (2)

- Blurred images have fewer dark pixels
 - If x is the dark pixel in a local patch of f
 - $g(x) = \sum_s h(s) f(x - s) \geq \sum_s h(s) \{ \min_{y \in \text{local patch}(x)} f(y) \}$
 $= \{ \min_{y \in \text{local patch}(x)} f(y) \} \sum_s h(s) = \{ \min_{y \in \text{local patch}(x)} f(y) \}$
 - $g(x) \geq f(x)$
 - The intensity values of dark pixel in f tend to become larger after the convolution

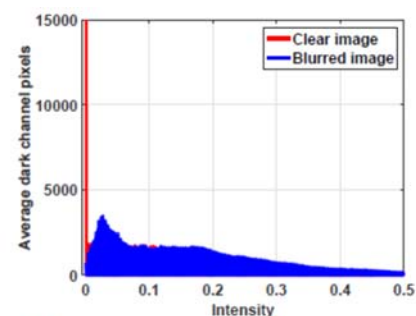
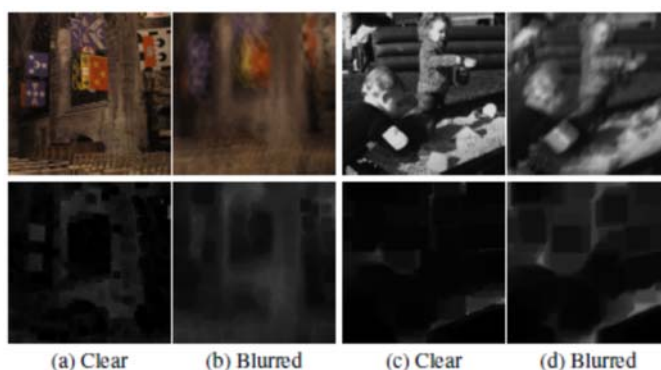


Figure 3. Intensity histograms for dark channels of both clear and blurred images in a dataset of 3,200 natural images. Blurred images have far fewer zero dark channel pixels than clear ones, confirming our analysis in the text. The dark channel of each image has been computed with an image patch size of 35×35 .

Deblurring Using Dark Channel Prior (3)

- Formulation

$$\min_{f,h} \|f * h - g\|_2^2 + \gamma \|h\|_2^2 + \mu \|\nabla f\|_0 + \lambda \|dark\ channel(f)\|_0$$

Regularize the solution of the blur kernel

Retain large gradients & remove tiny details

Enforce sparsity of dark channels



Figure 6. Visual comparisons using one challenging image from the dataset [16]. The deblurred images from other methods are from the reported results in [16]. The recovered image by the proposed algorithm with the dark channel prior is visually more pleasing.

Table 1. Quantitative evaluations on the text image dataset [26]. Our method outperforms several recent deblurring methods for natural images and is comparable to the method designed for text images [26].

	Cho and Lee [5]	Xu and Jia [34]	Krishnan <i>et al.</i> [17]	Levin <i>et al.</i> [20]	Xu <i>et al.</i> [36]	Pan <i>et al.</i> [26]	Ours
Average PSNRs	23.80	26.21	20.86	24.90	26.21	28.80	27.94

Image Editing & Resizing (1)

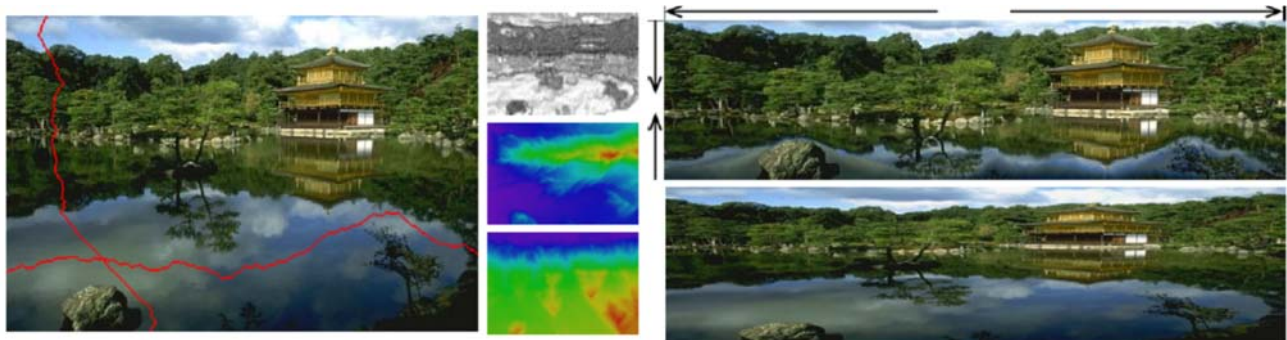
- Seam

- A connected path of low energy pixels of an image

- Seam carving

- Automatically carving out seams to reduce image size
 - Automatically inserting seams to extend image size

Content-aware resizing



- S. Avidan, and A. Shamir, "Seam Carving for Content-Aware Image Resizing," *ACM SIGGRAPH*, 2007.

Image Editing & Resizing (2)

- Given an $M \times N$ image $I(x, y)$
 - Vertical seam
 - An 8-connected path of pixels from top to bottom
 - Containing one (and only one) pixel in each row
 - $s^x = \{(x(1), 1), \dots, (x(N), N), \text{ s.t. } \forall i, |x(i) - x(i-1)| \leq 1\}$
 - where x is a mapping, $x: [1, \dots, N] \rightarrow [1, \dots, M]$
 - Horizontal seam
 - $s^y = \{(1, y(1)), \dots, (M, y(M)), \text{ s.t. } \forall j, |y(j) - y(j-1)| \leq 1\}$
 - where $y: [1, \dots, N] \rightarrow [1, \dots, N]$
- Goal
 - To look for an optimal seam that minimizes the seam cost
 - $s^* = \min_s E(s) = \min_s \sum_i e(I(s(i)))$
 - $e(I) = \left| \frac{\partial I}{\partial x} \right| + \left| \frac{\partial I}{\partial y} \right|$

Image Editing & Resizing (3)

To remove an object



To enlarge an image

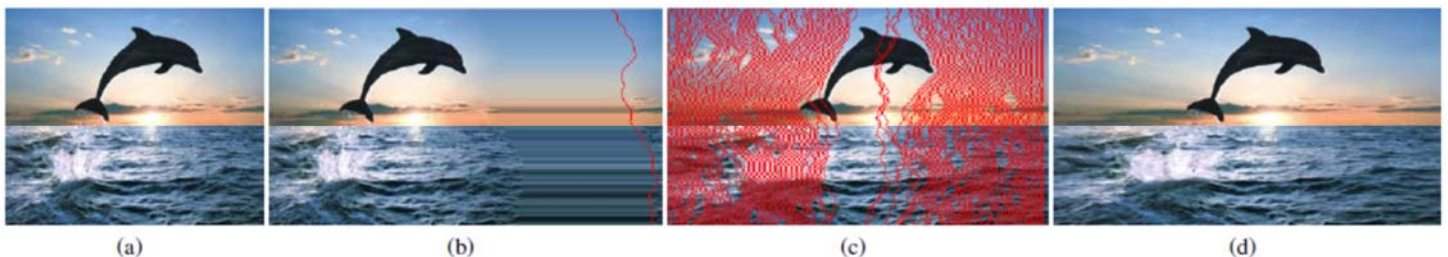


Figure 11: Simple object removal: the user marks a region for removal (green), and possibly a region to protect (red), on the original image (see inset in left image). On the right image, consecutive vertical seam were removed until no 'green' pixels were left.

Image Recomposition (1)

- Patch transform
 - An image is broken into non-overlapping patches
 - A modified image is reconstructed from the patches
 - Subject to user-specified constraints
 - Spatial location of patches
 - Size of the output image
 - The pool of patches used for reconstruction
 - The probability of all possible combination of patches
 - Adjacent patches should fit next to each other
 - Each patch should not be used more than once
 - The user's constraints should be maintained
 - Taeg Sang Cho, Moshe Butman, Shai Avidan, and William T. Freeman, "The patch transform and its applications to image editing," *Proc. 2008 IEEE Conference on Computer Vision and Pattern Recognition (CVPR)*.

Image Recomposition (2)



Figure 4. This example illustrates how the patch transform framework image. (b) The inverse patch transform result. Notice that the overall result. This figure shows that the proposed framework is insensitive of (b), a texture synthesis method by Efros and Leung [10] is used to

To recenter a region of interest

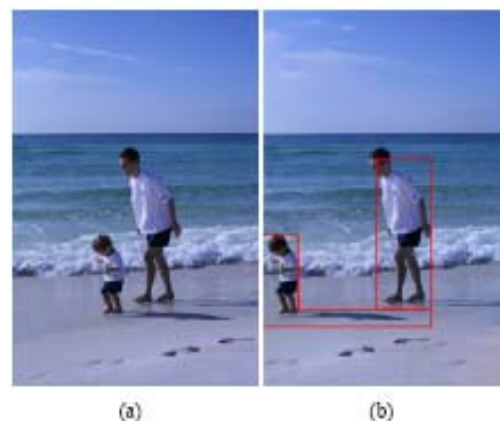


Figure 5. This example shows that the proposed framework can be used to change the relative position of multiple objects in the image. (a) The original image. (b) The inverse patch transform result with a user specified constraint that the child should be placed further ahead of his father.

Image Recomposition (3)

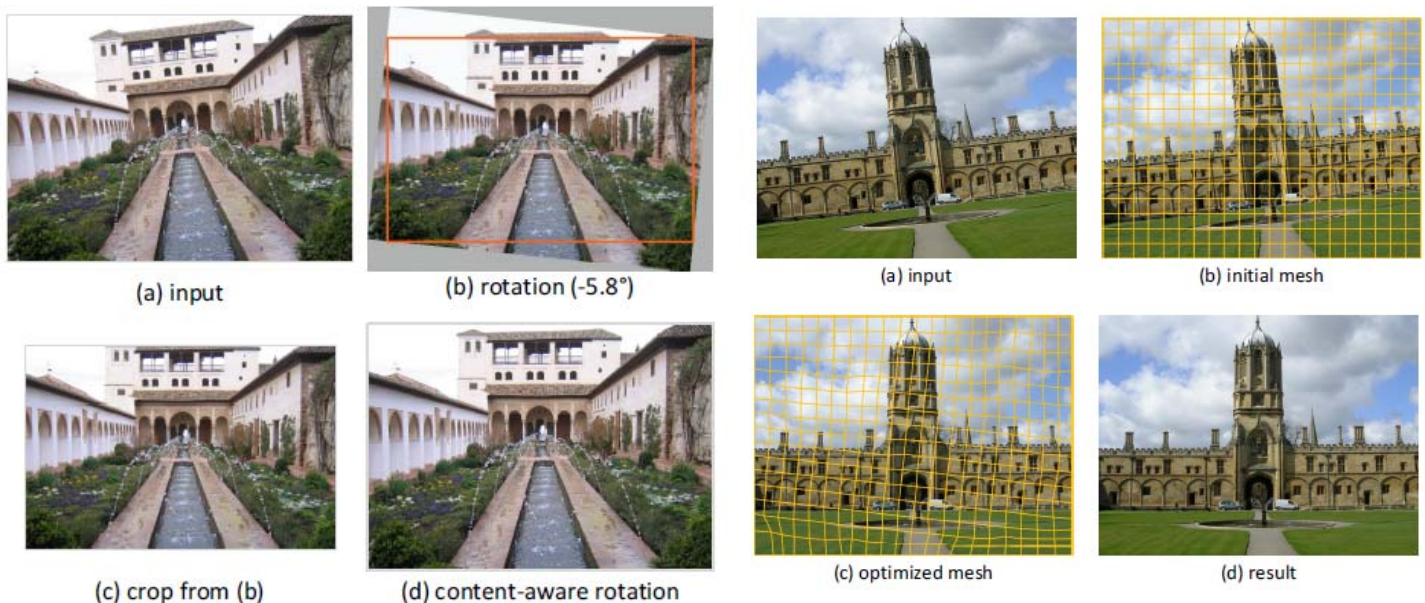


Figure 8. In this example, the original image shown in (a) is resized such that the width and height of the output image is 80% of the original image. (b) The reconstructed image from the patch transform framework. (c) The retargeting result using *Seam Carving* [2]. While *Seam Carving* preserves locally salient structures well, our work preserves the global context of the image through local evidence.



Figure 9. In this example, we collage two images shown in (a) and (b). (c) The inverse patch transform result. The user wants to copy the mountain from (b) into the background of (a). The new, combined image looks visually pleasing (although there is some color bleeding of the foreground snow.) (d) This figure shows from which image the algorithm took the patches. The green region denotes patches from (a) and the yellow region denotes patches from (b).

Content-Aware Rotation



- K. He, H. Chang, and J. Sun, “Content-Aware Rotation,” in *Proc. ICCV*, 2013.

Exposure Fusion

Short exposure image



(a)



Long exposure image

(b)

Fusion result



- M. Bertalmio, and S. Levine "Variational Approach for the Fusion of Exposure Bracketed Pairs", *IEEE Trans. Image Processing*, vol. 22, no. 2, Feb. 2013, pp. 712-723.

Semantic-Aware Sky Replacement (1)

- Automatic background replacement
 - Segmentation of sky region
 - Sky search
 - Search photos with similar layout from 415 high quality images
 - Sky replacement & appearance transfer to fg



Input photograph



Automatic sky replacement results with different styles

- Yi-Hsuan Tsai, Xiaohui Shen, Zhe Lin, Kalyan Sunkavalli, and Ming-Hsuan Yang, [Sky is Not the Limit: Semantic-Aware Sky Replacement](#), **SIGGRAPH**, July, 2016.

Semantic-Aware Sky Replacement (2)

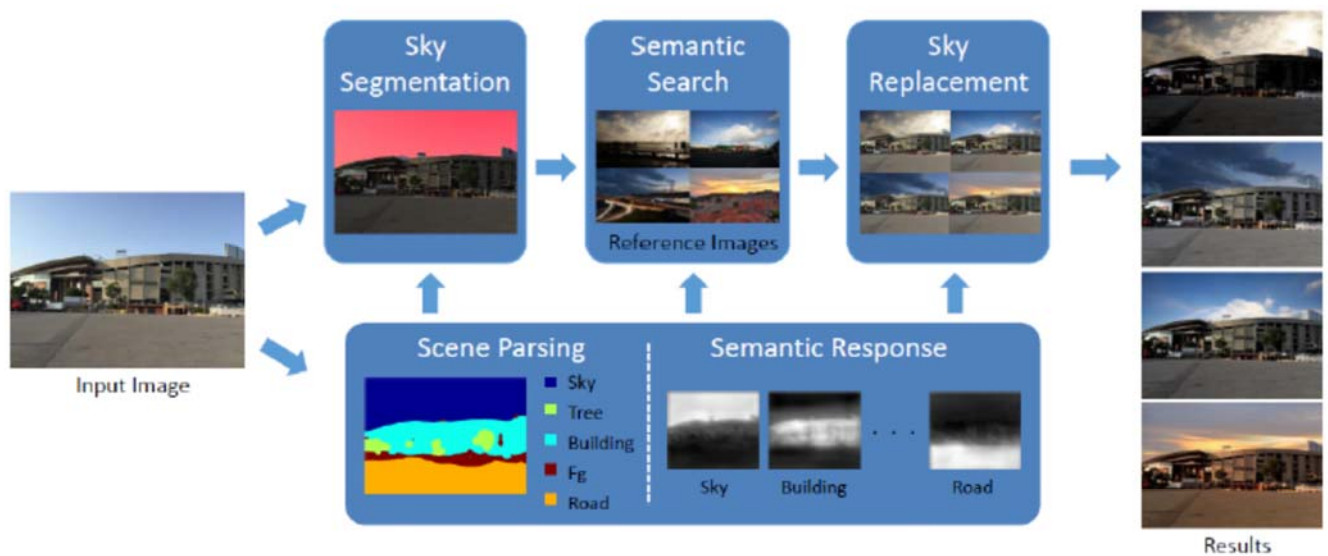
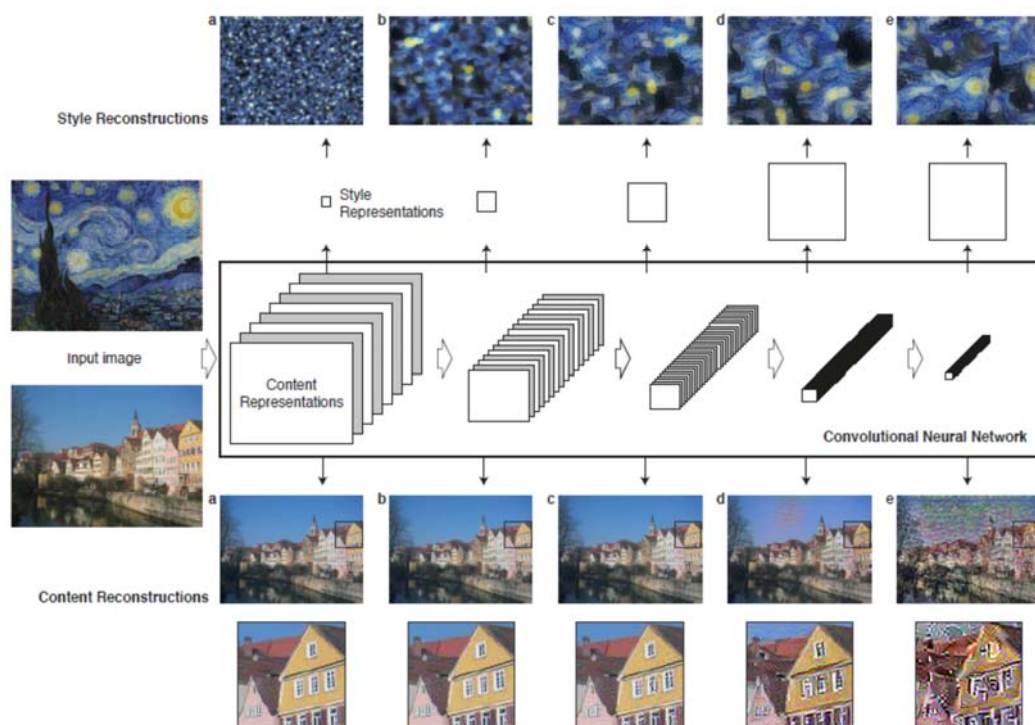


Figure 2: Overview of the proposed algorithm. Given an input image, we first utilize the FCN to obtain scene parsing results and semantic response for each category. A coarse-to-fine strategy is adopted to segment sky regions (illustrated as the red mask). To find reference images for sky replacement, we develop a method to search images with similar semantic layout. After re-composing images with the found skies, we transfer visual semantics to match foreground statistics between the input image and the reference image. Finally, a set of composite images with different stylized skies are generated automatically. Photo credits: Scott Cohen, PokoPoko, Yikuen Tsai, Alex and Danny Molyneux.

Style Transfer (1)



- L.A. Gatys, et al. Image Style Transfer Using Convolutional Neural Networks, in CVPR 2016

Style Transfer (2)

- To synthesize an image x
 - Given a content image p and a style image a
 - Minimizing the loss function

$$\mathcal{L}_{\text{total}}(\vec{p}, \vec{a}, \vec{x}) = \alpha \mathcal{L}_{\text{content}}(\vec{p}, \vec{x}) + \beta \mathcal{L}_{\text{style}}(\vec{a}, \vec{x})$$

- Matching the content representation of p
- Matching the style representation of a

